

## Bond percolation on a dilute lattice with short and long range correlations: A numerical simulation

Ulf Bauerschäfer

*Fachbereich Physik, Universität Halle, 06099 Halle, Saale, Germany*

Michael Schulz

*Abteilung für Theoretische Physik, Universität Ulm, 89069 Ulm, Germany*

(Received 19 October 1995)

The quenched percolation problem on a dilute lattice with a given random structure of vacancies is analyzed by numerical simulations in  $d=2$  and  $d=3$ . The distribution of the sites of the dilute lattice satisfies the static structure factor  $S(k) = ak^{-2} + b$  and contains short range ( $a=0$ ) and long range ( $a \gg 0$ ) effects, respectively. The numerical simulation shows that the critical behavior of the percolation on lattices with short range correlations ( $a=0$ ) is equivalent to the usual percolation on a regular lattice, whereas the percolation on a lattice with long range correlations shows a characteristic change of the universality class. In particular, a critical exponent  $\beta$  was detected, which is significantly greater than the usual exponent  $\beta_{random}$ . [S1063-651X(96)09706-1]

PACS number(s): 05.50.+q, 02.70.Lq, 05.70.Jk

### I. INTRODUCTION

The formation of molecular networks (for instance the formation of a gel starting from monomers) can be described in an obvious way by using the percolation concept. The classical percolation model is based on a regular lattice (translation symmetry). The lattice site corresponds to monomers, whereas lattice links are latent bonds. In the course of the network formation these latent bonds are transformed into real bonds. Thus, the occupation probability  $p$  (fraction of occupied links) is the usual measure for the closed chemical bonds. Analytical [1,2] and numerical [3] investigations show the well known critical behavior near the sol-gel transition.

On the other hand, many network formation processes are realized on lattices, where only a part of the lattice points is occupied by monomers, i.e., we have a dilute lattice. For instance, such a situation is given by various versions of the interpenetrating network (IPN) formation, e.g., if a polymer network of component A is swollen by monomers of a second component B. If this system has reached the equilibrium state, the formation of the subnetwork B is started by an external initialization (e.g., radiation initialization). Thus the formation of B can be interpreted as a percolation procedure on a diluted lattice (note that the vacancies of such a dilute lattice are these sites, which are occupied by monomers of type A).

The simplest case is the bond percolation on a dilute lattice [4-7] with a random distribution of the available lattice sites, i.e., a lattice site is occupied by a vacancy with the probability  $\rho$  independent on another sites, i.e., the density of free lattice sites is given by  $1-\rho$  (see Fig. 1). Thus, one obtains a set of inaccessible bonds (which are neighbored at least to one vacancy) and the percolation procedure is confined to the remaining latent bonds (such bonds connect two neighbored lattice sites, which are not occupied by vacancies). A more general situation in comparison to the percolation on a random dilute lattice is given by an inhomogeneous

spatial distribution of free lattice sites. The inhomogeneity can be characterized by the well known static structure factor  $S(k)$ , which is a usual characteristic quantity of the lattice disorder.

The following considerations are confined to the numerical simulation of two types of disorder, i.e., short range disorder

$$S(k) \sim \text{const} \tag{1}$$

and long range disorder

$$S(k) \sim \frac{1}{k^2} \tag{2}$$

of available sites. The most famous example of the presently

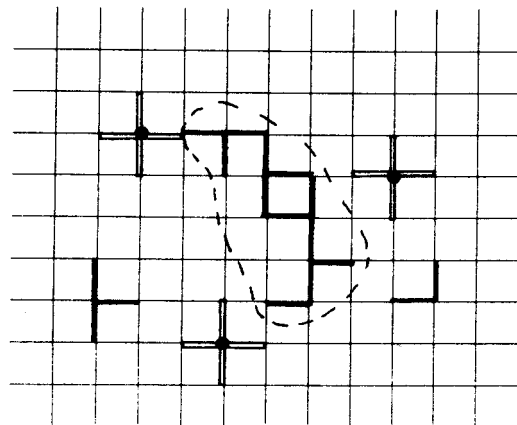


FIG. 1. Cluster on the square lattice for the bond percolation problem with defects. A lattice site is occupied (dots) by a vacancy (defect) with probability  $\rho$  (density of vacancies). Such a defect is neighbored by prohibited bonds (double line), which cannot be occupied by a real bond during the percolation procedure. All other bonds can be occupied with the probability  $p$  (thick lines) or empty (thin lines).

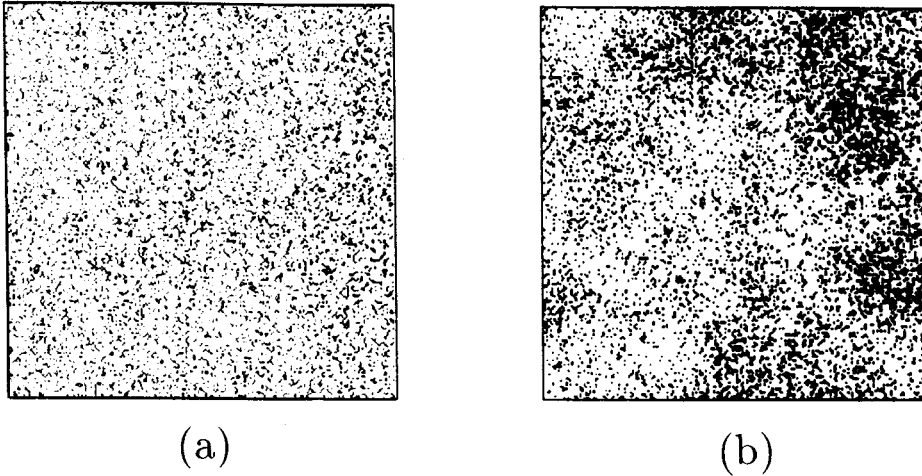


FIG. 2. Examples for configuration of defect distribution on a  $200 \times 200$  square lattice. Occupied sites of the bond lattice (defects) correspond with dots. (a) shows a random distribution of defects, (b) presents the same situation [(a)] after the optimization with respect to the static structure factor  $S = a/k^2 + b$ ,  $a \approx 7.5 \times 10^7$ .

studied long range and short range disorder is the Ising model: at the critical point the correlation function of parallel spins decays with a power law similar to (2).

Short range disorder [4] has the same percolation behavior as the usual percolation on a regular lattice, whereas a new universality class [8] was predicted for the percolation on a dilute lattice with long range correlations.

An  $\epsilon$  expansion ( $\epsilon = 6 - d$ ) near the critical dimension  $d_c = 6$  in terms of the renormalization group approach leads to the following representation of the critical indices under consideration of the two cases of disorder:

critical indices	classical (Caley tree)	short range disorder	long range disorder
$\eta$	0	$-\frac{1}{21}\epsilon + o(\epsilon^2)$	$o(\epsilon^3)$
$\nu$	$\frac{1}{2}$	$\frac{1}{2} + \frac{5}{84}\epsilon + o(\epsilon^2)$	$\frac{1}{2} + \frac{1}{8}\epsilon + o(\epsilon^2)$
$\beta$	1	$1 - \frac{1}{7}\epsilon + o(\epsilon^2)$	$1 + o(\epsilon^3)$
$\gamma$	1	$1 + \frac{1}{7}\epsilon + o(\epsilon^2)$	$1 + \frac{1}{4}\epsilon + o(\epsilon^2)$
$\alpha$	-1	$-1 + \frac{1}{7}\epsilon + o(\epsilon^2)$	$-1 - \frac{1}{4}\epsilon + o(\epsilon^2)$
$\delta$	2	$2 + \frac{2}{7}\epsilon + o(\epsilon^2)$	$2 + \frac{1}{4}\epsilon + o(\epsilon^2)$
$\sigma$	$\frac{1}{2}$	$\frac{1}{2} + o(\epsilon^2)$	$\frac{1}{2} - \frac{1}{16}\epsilon + o(\epsilon^2)$
$\tau$	$\frac{5}{2}$	$\frac{5}{2} - \frac{1}{14}\epsilon + o(\epsilon^2)$	$\frac{5}{2} - \frac{1}{16}\epsilon + o(\epsilon^2)$

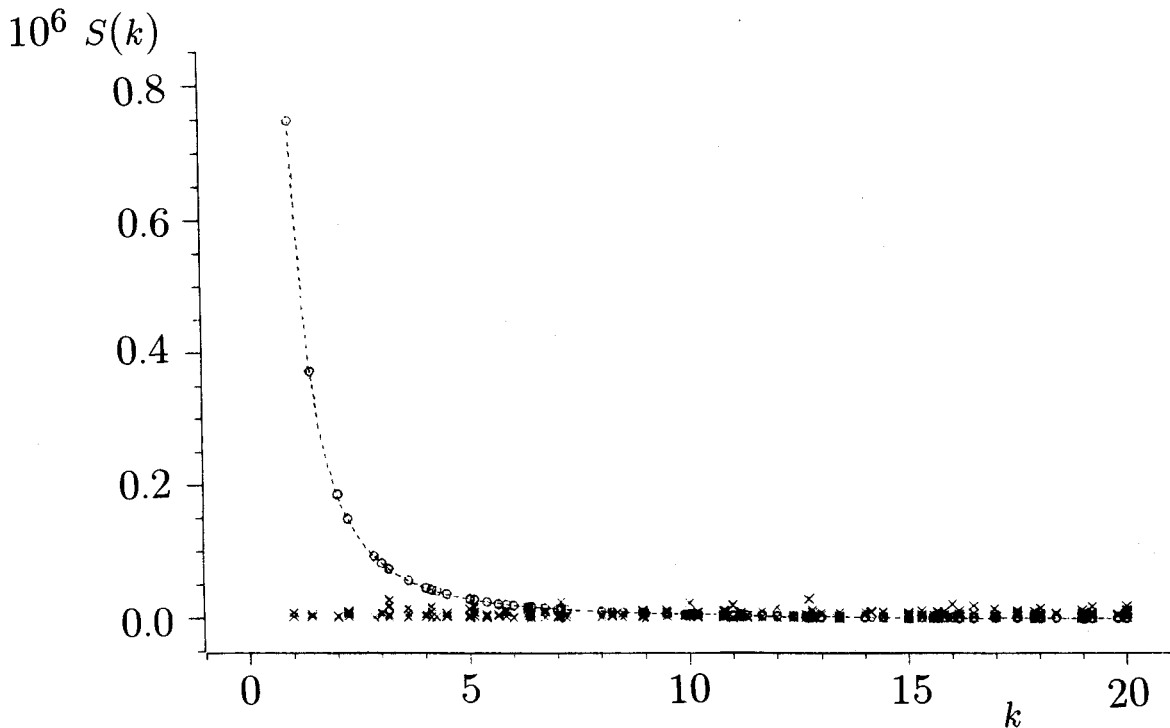


FIG. 3. Structure factor of Fig. 2(a) ( $\times$ ) and Fig. 2(b) ( $\circ$ ); the broken line  $--$  is a fit for  $S(k)$  with the two free parameters  $a$  and  $b$  [see Eq. (3)].  $k$  is the length of the wave vector.

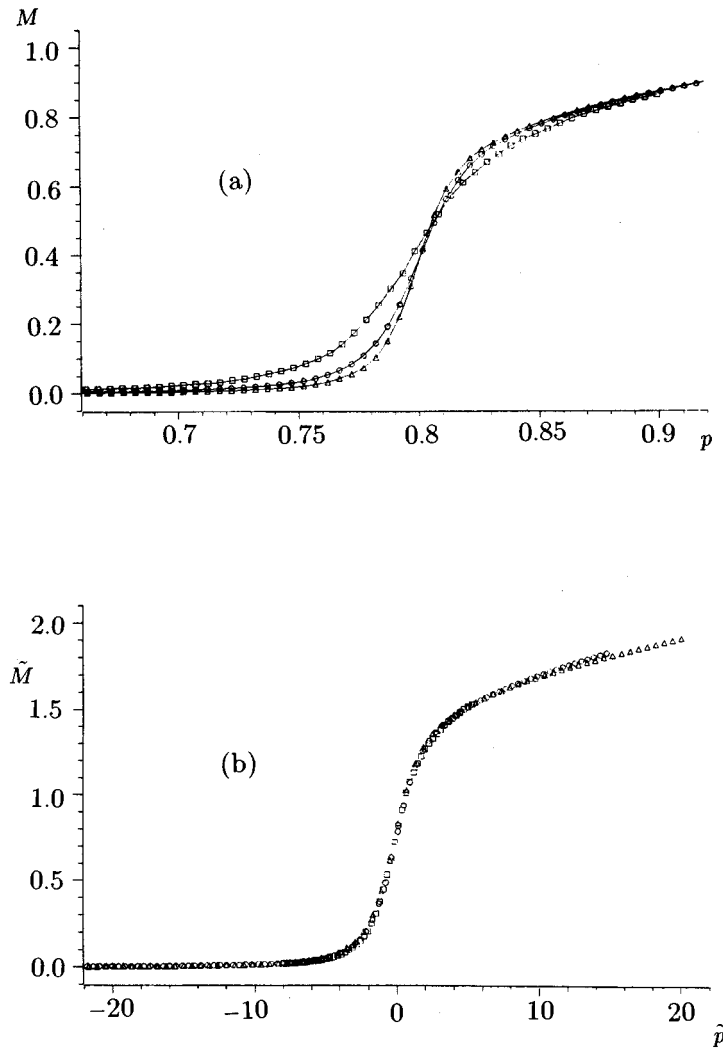


FIG. 4. (a) Finite-size scaling plots for the mass of the infinite cluster  $M(p)$  on a lattice with a defect concentration  $\rho=0.3$ .  $p$  is the occupation probability,  $L=200$  ( $\square$ ),  $L=400$  ( $\circ$ ), and  $L=600$  ( $\triangle$ ); (b)  $\tilde{M}=L^{\beta/\nu}M(p)$  is plotted versus  $\tilde{p}=(p-p_c)L^{1/\nu}$  with the exponents  $\beta=0.14$  and  $\nu=1.33$

The aim of this paper is the numerical verification of renormalization group for the percolation on dilute lattices with long range disorder in two and three dimensions. Therefore, we use a bond percolation model on square ( $d=2$ ) and cubic ( $d=3$ ) lattices, respectively, with a stochastic distribution of free lattice sites [determined by the static structure factor  $S(k)$ , see Fig. 1]. Note that each vacancy excludes the nearest neighbored bonds of the lattice from the percolation procedure and changes the original topology of the bond lattice.

Furthermore, we use the static structure factor  $S(k)$ :

$$S(k) = \frac{a}{k^2} + b \quad (3)$$

with the free parameters  $a$  and  $b$  and the wave vector  $k$ , which combines (1) and (2) to a more general representation. Note that  $k$  is here a dimensionless quantity, i.e., the wave vector is defined in terms of the lattice unit  $\ell$ :  $k\ell \rightarrow k$ .

## II. NUMERICAL GENERATION OF THE DISORDER

The generation of the lattice structure starts from a random distribution of defects and free lattice sites, respectively. Thus the static structure factor  $S(k)$  of the initial distribution of free sites corresponds to the functional structure (1), see Fig. 2(a). The positions of the vacancies are changed

by using a Metropolis algorithm [9] under the optimization condition that  $S(k)$  approaches the functional structure (3). This procedure consists in a series of elementary steps such that, starting from the initial configuration of free sites, further states are generated which are ultimately distributed according to the static structure factor (3). Note that an elementary step corresponds to a randomly chosen displacement of a randomly chosen vacancy, i.e., the total number of vacancies (and therefore the density of vacancies  $\rho$ ) is conserved.

Each elementary step leads to a change of the actual static structure factor. The deviation from the desirable final static structure factor (3) with given parameters  $a$  and  $b$  can be described by the measure

$$Q = \sum_k \left[ S_{ac}(k) - \left( \frac{a}{k^2} + b \right) \right]^2.$$

If the static structure factor after one elementary process approaches the final functional form (3), i.e.,  $Q_{new} < Q_{old}$ , the new configuration is accepted, otherwise the new configuration is rejected with a probability  $1 - \exp\{(Q_{old} - Q_{new})/T\}$ . The ‘‘temperature’’ is the control parameter of the procedure, which decreases very slowly during the Metropolis algorithm. Note that this decreasing is similar to a simulated

annealing of thermodynamical systems, which leads finally to a freeze in of the ground state.

However, the aim of the presented Metropolis algorithm is the realization of the minimum mean square deviation of the actual static structure factor  $S_{ac}(k)$  with respect to the static structure factor (3),

$$\sum_k \left[ S_{ac}(k) - \left( \frac{a}{k^2} + b \right) \right]^2 \rightarrow \min. \quad (4)$$

It is convenient to realize the optimization by the following two subroutines:

(i) The first part of the optimization procedure considers only the long range correlations (low  $k$ ); short scales are ignored. (ii) After reaching a satisfactory functional structure of  $S_{ac}(k)$  for the long range correlations, the optimization of the short scale structure is realized.

The result is a stochastic structure of the dilute lattice with long range correlations [Fig. 2(b)]. Figure 3 shows the static structure factor for randomly distributed free sites (used as initial configuration) and the same system after realization of the optimization procedure.

### III. PERCOLATION

The bond percolation procedure was simulated on a dilute lattice (with a given static structure factor) taking into account free boundary conditions. All averages are realized over 20 different defect distributions (quenched average) with the same static structure factor (3) and over 100 various percolation configurations for each actual defect structure. The mass  $M(p)$  of the infinite percolation cluster and the second moment

$$M_2(p) = \frac{\sum_n c_n n^2}{\sum_n c_n n}$$

( $c_n$  is the concentration of clusters with the mass  $n$ ) are computed as a function of the occupation density  $p$  (with respect to the total number of latent bonds). Note that  $p$  is the control parameter of the bond percolation growth process.

The results of the percolation on a diluted lattice with short range defect correlation (random diluted lattice) are well known [4], and we use this version as a test of the numerical algorithm and as a reference model in comparison to the bond percolation on a lattice with long range correlations. As expected, the random distribution of available lattice sites shows no influence to the critical indices. This conservation of the universality class was illustrated by the case of a two-dimensional dilute lattice with a concentration of defects  $\rho=0.3$ . Figure 4(a) shows  $M(p)$  for different lattices sizes  $L=200$ ,  $L=400$ , and  $L=600$ . The finite size scaling [10]

$$\tilde{p} = (p - p_c) L^{1/\nu}, \quad (5)$$

$$\tilde{M} = M L^{\beta/\nu}, \quad (6)$$

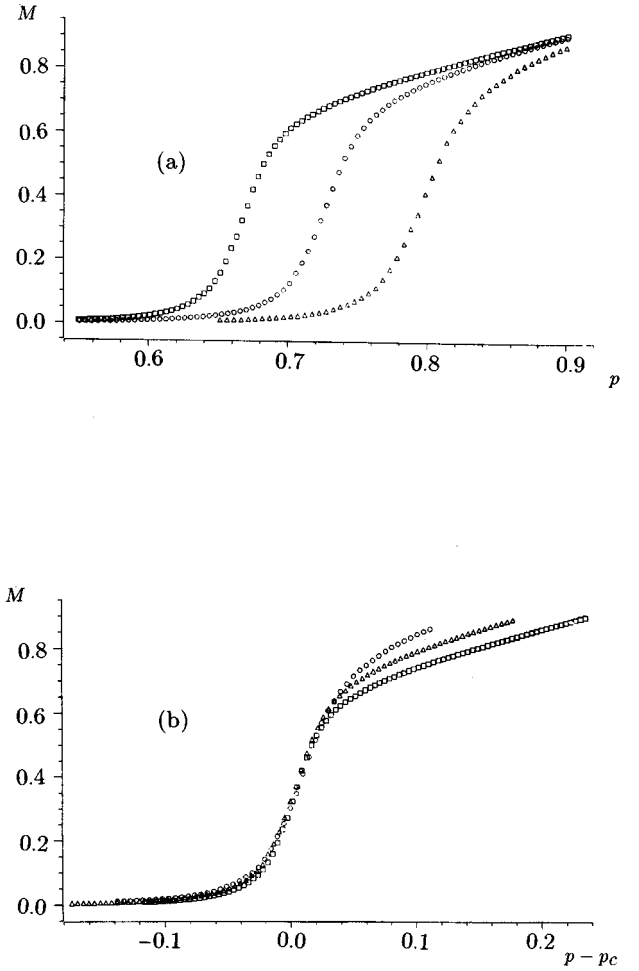


FIG. 5. (a) Effect of variation of the defect concentration  $\rho$  on the percolation probability on a square lattice with  $L=200$ ;  $\square$ :  $\rho=0.2$ ;  $\circ$ :  $\rho=0.25$ ;  $\Delta$ :  $\rho=0.3$ ;  $L=200$ . (b)  $M(p)$  is plotted versus  $p - p_c$  of the data from (a).

with the critical indices  $\beta$  and  $\nu$  [3] of the usual percolation problem leads a good superposition [Fig. 4(b)]. Only the nonuniversal percolation threshold  $p_c$  is under the influence of the random dilution.

The variation of the defect density  $\rho$  corresponds also only to a change of  $p_c$ , see Fig. 5(a). After a reshift  $\Delta p = -p_c$  of the functions  $M(p)$  we obtain an equivalent behavior near  $p - p_c = 0$ . Clearly, different defect densities lead to different lattice topologies. This is the origin for the splitting of the master curves above  $p_c$ .

Figure 6 shows the influence of the parameter  $a$  [long range defect distributions, Eq. (3)]. We present here the mass of the infinite cluster  $M(p)$  on a  $200 \times 200$  lattice with a defect concentration  $\rho=0.2$  for an increasing  $a$ . The slope near  $p_c$  decreases with increasing  $a$ , reaches a minimum at  $a_{opt}$ , and increases for higher  $a$ . Note that for  $a > a_{opt}$  the mass  $M(p)$  converges for  $p \rightarrow 1$  to a new limit [Fig. 6(a)]. The same effect is observable for the second moment of the cluster size distribution  $M_2(p)$  (weight averaged molecular weight of the sol fraction), where the maximum of  $M_2(p)$  was shifted to lower values at  $a > a_{opt}$ . Furthermore, for  $a > a_{opt}$  and  $p \rightarrow 1$ ,  $M_2(p)$  converges to a finite value, whereas  $M_2(p)$  vanishes for small  $a (a < a_{opt})$  and  $p \rightarrow 1$

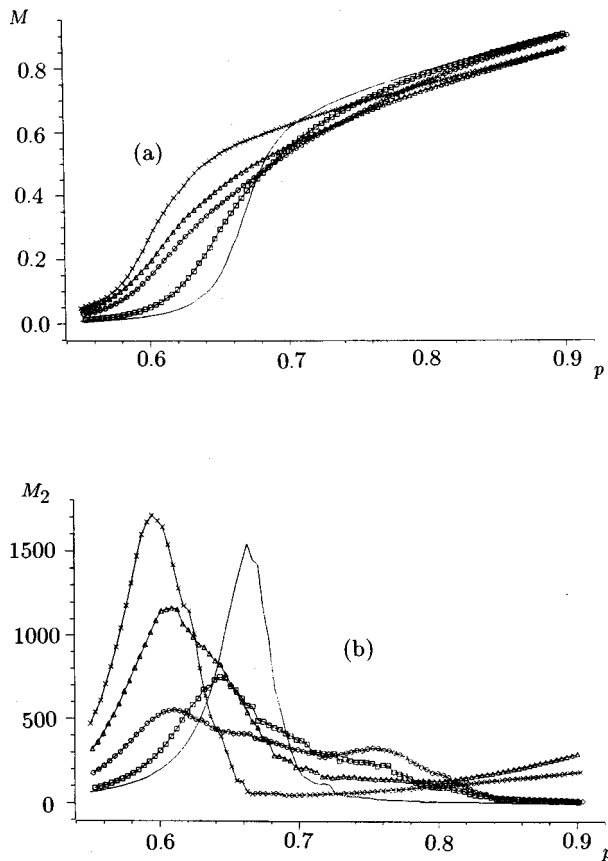


FIG. 6. Influence of different defect distributions (given by the variation of the parameter  $a$ ) to  $M(p)$  (a) and  $M_2(p)$  (b) on a lattice with fixed  $L=200$  and  $\rho=0.3$ : The parameter  $a$  is given by  $a=0.0$  (random distribution, full line),  $a=2.5 \times 10^7$  ( $\square$ ),  $a=7.5 \times 10^7$  ( $\circ$ ),  $a=15.0 \times 10^7$  ( $\Delta$ ), and  $a=30.0 \times 10^7$  ( $\times$ ).

[Fig. 6(b)]. This fact indicates the special meaning of  $a_{opt}$ , which corresponds to the minimum slope the slope of  $M(p)$  near  $p_c$ . For  $a < a_{opt}$  the defects disturb only lattice structure, but there exist no large isolated clusters of free lattice sites. Thus, the infinite cluster of the bond percolation behaves like the infinite cluster on a regular lattice. For  $a > a_{opt}$ , high density areas of defects cut large single clusters from the infinite cluster permanently, i.e., the topological connectivity of the lattice is violated. The result is an increasing number of isolated clusters (with a relative small number of defects in the bulk) for  $p \rightarrow 1$ . This leads to the further conclusion that the infinite cluster (or better the cluster which connects the surfaces of the finite simulation volume) grows near  $p_c$  for sufficiently high  $a > a_{opt}$  in the same way as  $M(p)$  for total randomly distributed defects ( $a=0$ ), and only the percolation threshold is shifted [Fig. 6(a)].

Therefore, a dilute lattice with long range correlations and without a violation of the connectivity is obtained for  $a \approx a_{opt}$ . In the present example we have  $a_{opt} = 7.5 \times 10^7$ .

For the following simulations we use defect configurations with  $\rho=0.3$  ( $d=2$ ) and  $\rho=0.6$  ( $d=3$ ) and a parameter  $a \approx a_{opt}$ . The percolation procedures are realized in two and three dimensions with field sizes  $600 \times 600$  and  $30 \times 30 \times 30$ , respectively. Figures 7 and 8 show  $M(p)$  and  $M_2(p)$  for structured lattices (long range correlation of the free lattice sites) with  $a \approx a_{opt}$  in comparison to the percola-

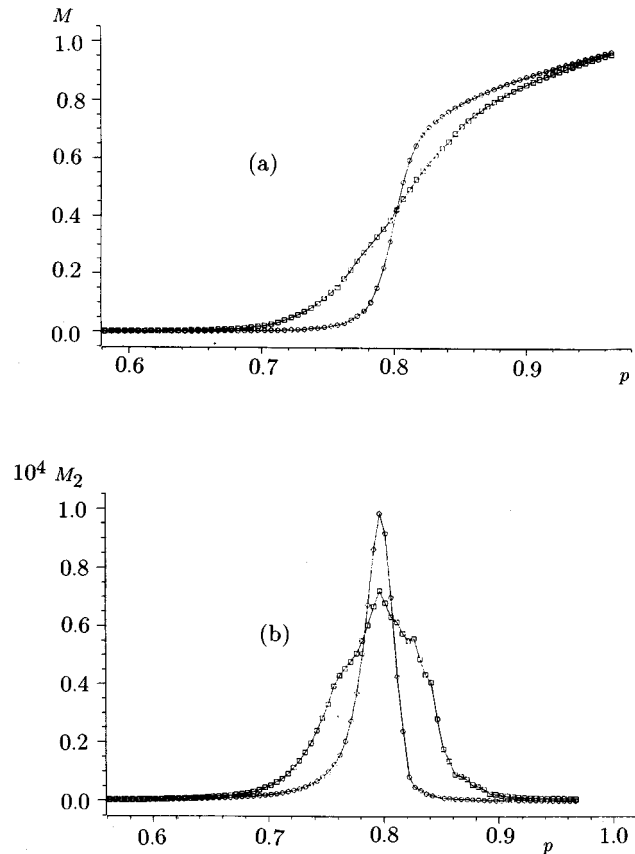


FIG. 7. Two-dimensional percolation with minimal slope near  $p_c$  [ $L=600$ ,  $\rho=0.3$ , average over 15 distributions of defects (quenched average), with 50 percolation sweeps per structure].  $M(p)$  (a) and  $M_2(p)$  (b) are represented for random ( $\circ$ ) and long range structure ( $\square$ ).

tion with random distributed defects ( $a=0$ ).

For the computation of the critical exponent  $\beta$  (which determines the scaling behavior of the infinite cluster mass) we use the typical scaling region, indicated by the region between the maximum and the onset of the foot of the second moment  $M_2(p)$ . Figure 9 shows a three parameter fit of the mass  $M(p)$  in this region by using the scaling function

$$M = c_0(p - p_c)^\beta.$$

The percolation on a random diluted lattice is determined [Fig. 9(a)] by the approach

$$\beta_{random} = 0.2 \pm 0.1 \quad (d=2)$$

and [Fig. 9(b)]

$$\beta_{random} = 0.5 \pm 0.1 \quad (d=3).$$

Clearly, the error bars are very high, but a finite size scaling [3] leads to the more serious results  $\beta_{random} = 0.14 \pm 0.01$  ( $d=2$ ) and  $\beta_{random} = 0.4 \pm 0.02$  ( $d=3$ ). Note that a maximum length  $L=600$  ( $d=2$ ) and  $L=50$  ( $d=3$ ), respectively, is sufficient enough to obtain these values and the corresponding error bars. This result is in good agreement with the well known results [4], e.g., the critical exponents for the percolation on a random diluted lattice and on a nondilute lattice are the equivalent.

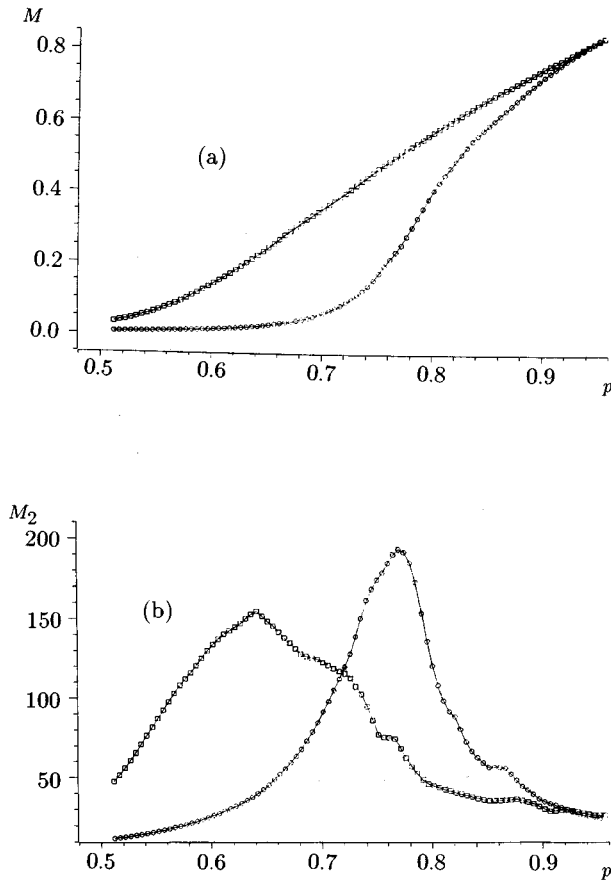


FIG. 8. Three-dimensional percolation with  $L=30$ ,  $\rho=0.3$  (average over 30 defect configurations with 100 percolation sweeps per structure) for  $M(p)$  (a) and  $M_2(p)$  (b) for random ( $\circ$ ) and long range structure ( $\square$ ).

Figures 7 and 8 show the significant influence of the long range correlation of the dilute lattice to the scaling behavior of  $M(p)$  and  $M_2(p)$ .  $M(p)$  grows above  $p_c$  approximately with

$$\beta_{struc} = 0.4 \pm 0.1 \quad (d=2) \quad (7)$$

and

$$\beta_{struc} = 0.9 \pm 0.1 \quad (d=3). \quad (8)$$

These results correspond also to the finite size approximation, but the stability of this method is weak in comparison to the case of a random dilute lattice with short range correlations, i.e., the error bars are of the same order as in the simple approach (7) and (8).

A higher precision is only possible by using larger length. On the other hand, the computation time for the Metropolis

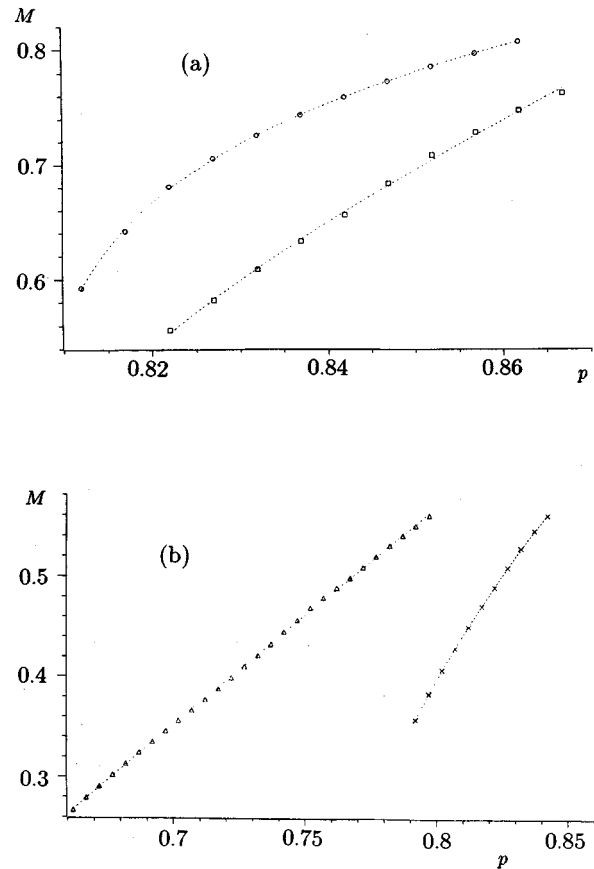


FIG. 9. Fit of  $M(p)$  for Fig. 7(a) and Fig. 8(a). (a)  $d=2$  with random ( $\circ$ ) and long range defect distribution ( $\square$ ); (b)  $d=3$  with random ( $\times$ ) and long range defect distribution ( $\Delta$ ).

algorithm [9] (which was used for creation of the long range correlated structure) increases rapidly with increasing  $L$ . From this fact  $L=600$  ( $d=2$ ) and  $L=50$  ( $d=3$ ) are a reasonable optimum length for the numerical calculation of the critical exponents. The results (7) and (8) indicate a characteristic change of the scaling behavior and therefore of the universality class between the behavior on a dilute lattice with long range distribution of the free sites to a random diluted lattice (short range correlations), which is the main result of this paper.

Clearly, the difference between the mass of the infinite clusters  $M(p)$  vanishes in both cases (long range and short range distribution of free lattice sites) for  $p \rightarrow 1$  (see Figs. 7 and 8), i.e., the influence structure of the lattice site distribution to the infinite cluster remains relevant only for large scales (which act near  $p_c$ ), which is how it was predicted in [8].

[1] D.J. Amit, J. Phys. A **9**, 1441 (1976).

[2] R.K.P. Zia and D.J. Wallace, J. Phys. A **8**, 1495 (1975).

[3] D. Stauffer and A. Aharony, *Introduction to the Percolation Theory*, 2nd ed. (Taylor and Francis, London, 1992).

[4] A. Coniglio, H.E. Stanley, and W. Klein, Phys. Rev. Lett. **42**, 518 (1979).

[5] M. Plischke, Phys. Rev. A **43**, 2056 (1991).

[6] E. Duering and D.J. Bergman, J. Stat. Phys. **60**, 363 (1990).

- [7] S.G.W. Colborne and A.J. Bray, *J. Phys. A* **22**, 2505 (1989).
- [8] M. Schulz, *J. Stat. Phys.* **67**, 1109 (1992).
- [9] N. Metropolis, A. Rosenbluth, M.N. Rosenbluth, A.H. Teller, and E. Teller, *J. Chem. Phys.* **32**, 1087 (1953).
- [10] K. Binder and D.W. Heermann, *Monte-Carlo Simulations in Statistical Physics, An Introduction*, Springer Series in Solid State Science (Springer, Berlin, 1988).